

# Optical Molasses Loaded From a Low-Velocity Intense Source of Atoms: An Atom Source for Improved Atomic Fountains

Elizabeth A. Donley, Thomas P. Heavner, and Steven. R. Jefferts, *Member, IEEE*

**Abstract**—We demonstrate the efficient capture of cesium atoms from a low-velocity intense source (LVIS) of atoms into an optical molasses. The high load rates that are achievable with the technique can potentially improve the stability of and reduce collisional shifts in atomic fountain clocks. An LVIS is an atomic beam created from a small hole in one of the retroreflectors in an otherwise ordinary magneto-optical trap (MOT). Our typical LVIS flux was  $10^{10}$  atoms/s. The asymptotic value for the number of atoms captured in the optical molasses was  $1.1(1) \times 10^9$  atoms, and the fill time constant was  $\tau = 290(30)$  ms. The initial molasses fill rate was  $R_{t=0} = 3.8(5) \times 10^6$  atoms/ms. At this rate, it would require 24 ms to capture and launch  $10^7$  state-selected atoms in an atomic fountain. The fill rate at short times indicates that approximately 40% of the LVIS atoms were being captured in the optical molasses.

**Index Terms**—Atomic beams, atomic clocks.

## I. INTRODUCTION

THE accuracy of primary frequency standards is limited by the uncertainties in the corrections of systematic frequency shifts. In the laser-cooled cesium atomic fountain NIST-F1, the limiting systematic uncertainties arise from corrections for the blackbody radiation shift and the spin-exchange shift. The next-generation fountain clock, NIST-F2, is being designed to reduce the size of these shifts and their related uncertainties [1].

To meet our goals of achieving an ultimate frequency inaccuracy of  $\delta f/f < 10^{-16}$ , the uncertainty of all of the systematic frequency shifts have to be reduced to well below the level of  $1 \times 10^{-16}$ . The largest uncertainty arises from the blackbody shift, and the size of that shift will be reduced for NIST-F2 by cooling the fountain microwave cavities and interrogation region to liquid nitrogen temperature. At a fractional frequency uncertainty of  $1.5 \times 10^{-16}$ , the uncertainty arising from correcting the spin exchange shift is presently the second largest in NIST-F1 [2]. Our efforts at reducing the uncertainty of the spin-exchange shift is the issue addressed here.

The primary frequency standard NIST-F1 is described in detail in [3]. Here, we describe the fountain operation only briefly. The relevant  $^{133}\text{Cs}$  transitions are indicated in the energy-level diagram in Fig. 1. The basic idea is that atoms from a  $^{133}\text{Cs}$  oven are collected in an optical molasses and launched upward with a velocity of about 4 m/s in a moving

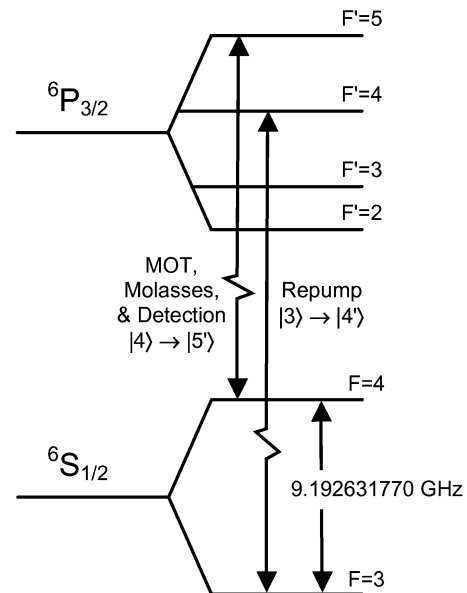


Fig. 1. Energy-level diagram for  $^{133}\text{Cs}$ . (Not to scale.) The fountain interrogates the ground-state hyperfine splitting at  $\sim 9.2$  GHz. The  $6^2S_{1/2} \rightarrow 6^2P_{3/2}$  optical transitions indicated by broken arrows are at a wavelength of  $\sim 852$  nm.

molasses. The atoms are initially distributed in all magnetic sublevels of the  $|F=4\rangle$  hyperfine ground state (nine levels). The ball of atoms first travels through a state-selection cavity where it is exposed to a  $\pi$  pulse of microwave radiation tuned to the  $|F=4, m_F=0\rangle \rightarrow |3, 0\rangle$  clock transition. The remaining  $|4, m_F \neq 0\rangle$  atoms are then removed from the sample with a pulse of light resonant with the  $|4\rangle \rightarrow |5'\rangle$  transition. While in flight, the ball of state-selected atoms is exposed to two pulses of microwave radiation—once while traveling upward through the Ramsey microwave cavity, and again on the way down through the same cavity. Then the transition probability is measured, and a subsequent ball of atoms is launched. The Ramsey interrogation occurs during the full time interval between microwave pulses.

With some minor variations in the details, this paradigm for the fountain mode of operation has been the standard approach for development of atomic fountains around the world, with the notable exceptions of a juggling  $^{87}\text{Rb}$  fountain [4] and a continuous-beam fountain that is under development [5].

This paper describes a continuation of work on the multiple-velocity fountain concept first proposed [6] and subsequently experimentally investigated [7] by Levi and coworkers.

Manuscript received March 31, 2004; revised February 7, 2005.

The authors are with the Atomic Standards Group, National Institute of Standards and Technology (NIST), Boulder, CO 80305-3328 USA.

Digital Object Identifier 10.1109/TIM.2005.853218

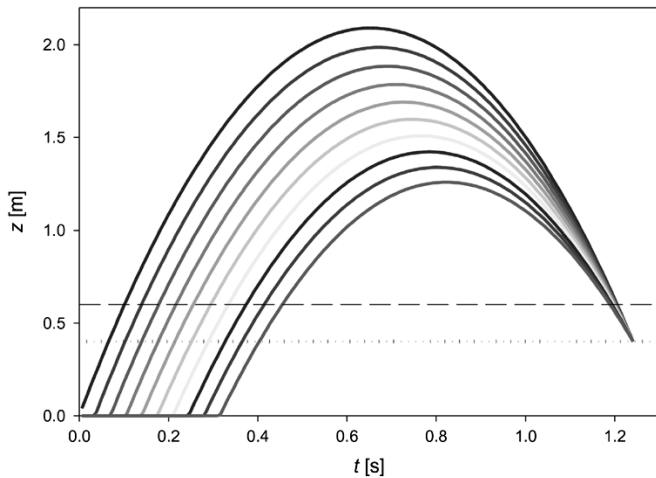


Fig. 2. Calculated trajectories for a multitoss scheme. The positions of the Ramsey cavity and the detection zone are shown as dashed and dotted lines, respectively. For this example, ten balls of atoms were launched at 35-ms intervals. The highest ball had an initial velocity of 6.4 m/s.

The method effectively reduces the density of the atomic sample by nearly an order of magnitude, and reduces the size of the spin-exchange shift by a comparable factor. The total atom number is maintained, and thus the fountain stability is not significantly compromised. The idea is to launch many balls in rapid succession, with each ball having a fraction of the number of atoms required to reach the target stability. Atom balls launched later in the sequence have lower apogees, such that no ball ever crosses paths with any other ball during the Ramsey interrogation. All balls meet in the detection zone and are detected simultaneously, thus reducing the significance of technical noise. Calculated trajectories for such a scheme of launching ten balls per measurement are shown in Fig. 2.

The multiple-velocity launch method relies on a high fill rate for the optical molasses. The optical molasses that was used for the initial demonstration of the multiple velocity fountain [7] was loaded from a Cs oven, which consisted of a conflat copper tube adapter containing cesium that was sealed closed. The tube of 1-cm diameter was positioned such that its axis intersected the molasses region and it was heated to  $\sim 40^\circ\text{C}$ . In this system, the fill rate was limited to  $\sim 1.6 \times 10^5$  atoms/ms at short times [8]. At this rate, it takes over 50 ms to load sufficient atoms to produce a sample of  $10^6$  state-selected atoms. We would like to load at least that many atoms in about 25 ms.

A low-velocity intense source (LVIS) of atoms [9] is a compact, high-flux, atomic beam source. A schematic drawing of an LVIS apparatus is shown in Fig. 3. The feature that distinguishes an LVIS apparatus from a standard magneto-optical trap (MOT) is the gold-coated quarter-wave plate with a hole drilled through its center that is used in place of one of the MOT beam retroreflectors. The hole casts a shadow through the MOT, creating an imbalance in the scattering rate from the forward- and backward-traveling laser beams. This creates a net force that accelerates the cold atoms through the hole and out of the trap. An LVIS of  $^{87}\text{Rb}$  atoms [9], [10] typically exhibits an atomic flux of order  $10^{10}/\text{s}$ , a tunable axial velocity of order 15 m/s with a narrow velocity spread of order 2 m/s, and transverse velocities of order 5 cm/s. Studies with cesium atoms have demon-

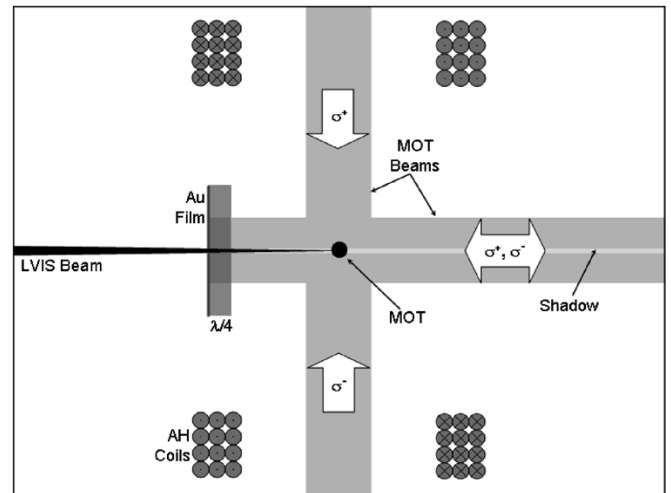


Fig. 3. Schematic drawing of the LVIS apparatus. A third pair of MOT laser beams perpendicular to the plane of the figure is not shown.

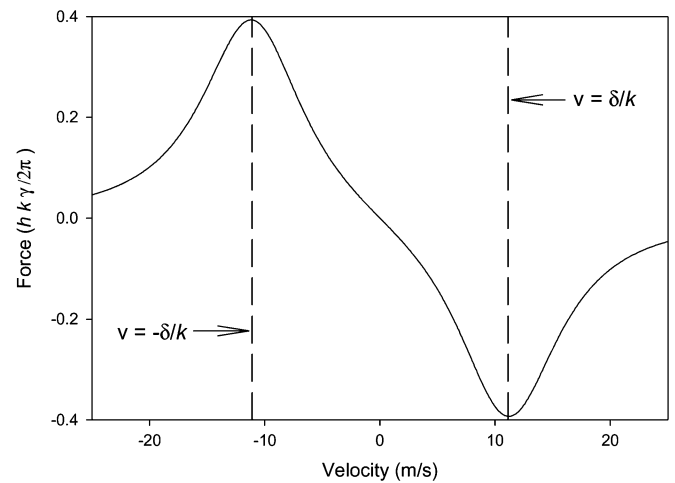


Fig. 4. Molasses capture force. The curve was calculated for a 1-D optical molasses with detuning  $2.5\gamma$  and a saturation parameter  $I/I_{\text{sat}} = 5$ , where  $I_{\text{sat}}$  is the saturation intensity.

strated similar performance but with somewhat lower axial velocity (5–10 m/s), owing to the greater atomic mass of  $^{133}\text{Cs}$  [11].

With these properties, an LVIS is an ideal source for loading atoms into an optical molasses [12]. The capture force for typical values of the laser intensity and detuning in an optical molasses is shown versus the atomic velocity  $v$  in Fig. 4. For sufficiently large detuning, the capture force is peaked at a velocity of  $v = \pm\delta/k$ , where  $\delta$  is the laser detuning from the atomic resonance and  $k$  is the wavevector of the laser light. The intensity of the molasses beams determines the magnitude of the capture force. The low velocity and narrow velocity distribution of an LVIS beam combined with the molasses capture force versus velocity suggest that it should be possible to achieve a capture efficiency of nearly 100% for a beam of LVIS atoms into an optical molasses if sufficient laser power is available for the molasses beams.

Our primary objective for loading the molasses from an LVIS beam is the increased load rate. A bonus for reducing the molasses loading time is a reduction in dead time of fountain op-

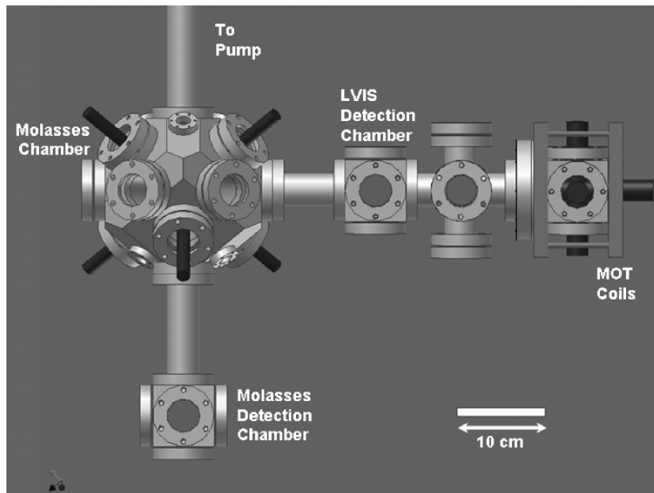


Fig. 5. Apparatus. For simplicity, the molasses and MOT beams are shown as cylinders protruding through the vacuum flanges. The scale is indicated by the 10-cm bar on the lower right.

eration. Even for a fountain running in the standard single-ball launch mode, reduction of the dead time between interrogations improves the stability directly by reducing the cycle time. The stability degradation arising from the Dick effect [13] is also minimized by reducing the dead time.

Another advantage of loading a molasses from an LVIS is the tremendous gain in differential pumping ability. The thermal cesium source in an LVIS is far from the sensitive part of the vacuum system where background collisions are to be avoided, and the vacuum system can even be designed such that the MOT chamber is connected to the fountain vacuum system only through the 0.5-mm diameter hole in the LVIS mirror through which the LVIS beam emerges. All of the cesium atoms that reach the molasses region are within the velocity range of being captured, thus there is relatively little ballistic cesium in the interrogation and detection regions, where it can limit the lifetime of the vacuum system, and it can generate excess scattered light into the detection system.

It should be noted that the generation of slow atomic beams is of considerable interest. A related review by Noh and Jhe presents an extensive section on the production of cold atomic beams [14].

## II. APPARATUS

A gold-coated quarter-wave plate of 5-cm diameter and with a hole of 0.5-mm diameter drilled through its center served as one of the MOT retroreflectors, and was mounted inside of the vacuum chamber in a custom 70-mm six-way cube cross at the right end of the apparatus, as shown in Fig. 5. To accommodate this custom optic in the vacuum chamber, a 114-mm con-flat flange was welded flush against one of the cube faces. To maximize the MOT load rate, the MOT trapping beams had a diameter of 2 cm ( $1/e^2$ ). This required the use of large-diameter (5-cm) polarizing optics. There were no magnetic-field trim coils on the MOT chamber. Instead, the anti-Helmholz coils were mounted to an x, y, z translation stage and the coils were moved to locate the trap center properly with respect to the shadow cast by the hole.

The atomic beam emerging through the hole in the gold-coated waveplate was measured and optimized in the LVIS detection chamber located 22 cm downstream from the MOT. A 1-mm-thick standing-wave light sheet tuned to the  $|F = 4\rangle \rightarrow |F' = 5\rangle$  cycling transition served as the detection beam. Repump light tuned to the  $|F = 3\rangle \rightarrow |F' = 4\rangle$  transition was overlapped with the detection light. The fluorescence was detected using a photodiode with a collection efficiency of  $1.5 \times 10^{-3}$  and amplified. This signal was fed to a lock-in amplifier. The fluorescence signal was modulated by chopping the repump light with a shutter. When the LVIS flux was maximized, it was possible to see the LVIS fluorescence from the detection beam with an infrared viewer, but lock-in detection was needed for optimization, since there were too many degrees of freedom to find the optimum settings by eye. When we initially found the LVIS signal, it was a few orders of magnitude weaker than when it was eventually optimized with  $\sim 10^6$  atoms in the detection beam.

The custom molasses vacuum chamber was built in the (1, 1, 1) geometry, which will allow for operation in the multiple-velocity fountain mode, since none of the molasses beams travel along the axis of the fountain drift tube (see Fig. 5). Laser light red-detuned from the  $|F = 4\rangle \rightarrow |F' = 5\rangle$  cycling transition was provided to the molasses through three fiber collimators that produced 1.0-cm diameter ( $1/e^2$ ) beams. Those beams were retro-reflected through quarter-wave plates to produce a lin  $\perp$  lin polarization arrangement.

For most of the measurements, atoms collected in the molasses were dropped and detected 25 cm below the center of the molasses chamber. The atoms fell through a standing wave light sheet that was 1-mm thick and resonant with the cycling transition, and their fluorescence was focused by a compound lens onto a photodiode (PD) with a high-gain amplifier. The detector was oriented perpendicular to the direction of propagation of the detection beams. We had difficulty obtaining an absolute load rate with this method because the atoms fell through a long graphite tube on their way to the detection zone, and a large fraction of the atom ball was skimmed off during the fall. The background pressure was also relatively high, and so at least half of the atoms were lost from collisions with background gas before they reached the detection zone. Because of these difficulties, the PD signal was calibrated by measuring the absolute number of atoms loaded into the molasses with two charge-coupled device (CCD) cameras that imaged the molasses directly. The camera responses were calibrated with a weak laser beam of known power, and the results from the different cameras were consistent.

## III. LVIS CHARACTERIZATION

The typical LVIS flux was  $10^{10}$  atoms/s. The optics did not require extensive realignment from day to day as long as the anti-Helmholz MOT coils were allowed to heat up completely, since thermal drifts were significant.

The required MOT field gradient was typical for a large MOT. The anti-Helmholz coils were coaxial with the LVIS beam and with the strong axis of the MOT trap. The LVIS flux began to saturate when the field gradient along the strong(weak) axis was

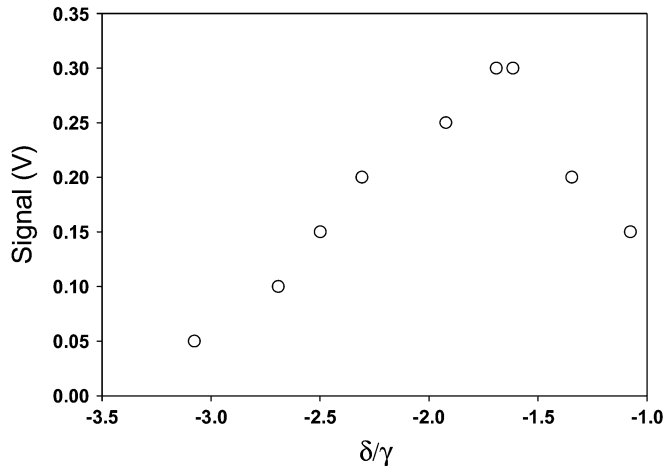


Fig. 6. LVIS signal versus laser detuning from resonance. The detuning is measured in linewidths.

70(35) mT/m. The total power required for the MOT beams was 100 mW.

As observed by Lu *et al.* [9], we observed that the LVIS flux was linear in MOT beam intensity up to a point, and at higher intensity, the LVIS signal saturated. The MOT beam intensity where the signal saturated was  $\sim 10$  mW/cm<sup>2</sup> per beam for our experiment, and  $\sim 40$  mW/cm<sup>2</sup> as measured by Lu and coworkers. For our experiment, the total laser power needed to reach saturation was  $\sim 100$  mW.

Considerable interest was generated by a study [15] that compared the performance of an LVIS, a two-dimensional (2-D)-MOT, and a 2-D<sup>+</sup>-MOT at much lower available laser power than was used in the original LVIS demonstration. The study used a total laser power of 34 mW and observed an LVIS flux of  $3 \times 10^8$  atoms/s, whereas the peak flux for the 2-D<sup>+</sup>-MOT configuration was nearly  $10^{10}$  for the same laser power. We observed an order of magnitude higher LVIS flux for the same laser power of 34 mW, which indicates that the LVIS technique may not compare as badly with the 2-D-MOT technique as was initially thought [15].

One difference between our LVIS implementation and those performed previously [9], [10] is that we observe the peak flux at a detuning of about  $2\gamma$ , whereas Lu *et al.* [9] observed the peak flux for <sup>87</sup>Rb atoms at a detuning of over  $5\gamma$ , where  $\gamma$  is the linewidth of the optical transition. Our flux versus detuning curve is shown in Fig. 6. Their flux versus detuning curve was about four times broader than what we observed. Wang and Buell [11] also observed a very broad flux versus detuning curve, and like us, they studied <sup>133</sup>Cs atoms. One difference between our measurements and these previous studies is that our LVIS beam escaped on the strong axis of our trap, whereas their LVIS beam escaped along one of the two weak axes. This affects how quickly the LVIS atoms are Zeeman-shifted out of resonance as they leave the trap. In our experiment, the atoms are shifted out of resonance twice as quickly. This experimental detail could make our LVIS beam less sensitive to deflection from intensity imbalances in the MOT beams. Interestingly, Camposeo and coworkers observed nearly exactly the same detuning

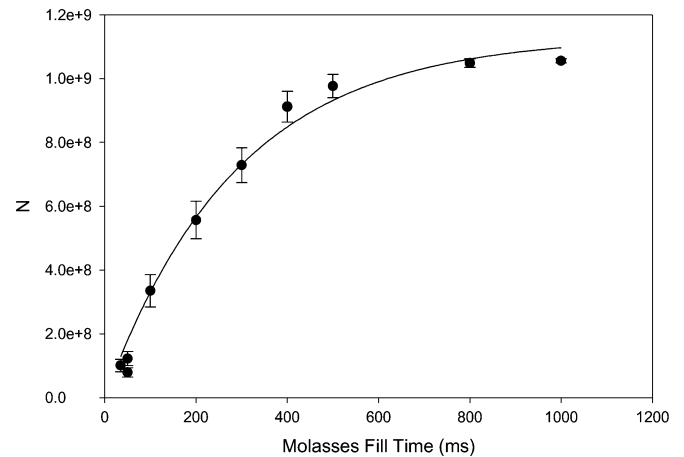


Fig. 7. Number of atoms captured in the optical molasses versus fill time. The  $N$ -axis has been calibrated with camera data. The error bars are errors estimated from the typical shot-to-shot variations in the load rate. Each individual point represents a single measurement. The error bars represent statistical uncertainties alone—calibration errors of the detection system could be larger, but are the same for all measurements.

dependence for the number of trapped cesium atoms in a pyramidal funnel configuration [16] as we observed for the LVIS flux.

The laser detuning that maximizes the number of trapped atoms in a MOT is  $3.2\gamma$ . We suspect that the reason that our flux was peaked closer to resonance is that the pressure on the MOT side of the LVIS mirror could have been as high as  $10^{-7}$  mbar for our experiment. A detuning closer to resonance results in a LVIS beam of higher velocity [9], [10], and thus the atoms spend less time in the region that has a higher collision rate. We did not measure the velocity of the LVIS beam directly, but in the next section, we infer the beam velocity based on the characterization of the optical molasses.

#### IV. OPTICAL MOLASSES CHARACTERIZATION

The molasses fill rate was very sensitive to the molasses detuning, the optimum value of which was  $2.5\gamma$ . The simulation of the one-dimensional (1-D) molasses capture force shown in Fig. 2 is based on the actual molasses parameters. Based on the modeled capture force and the measured detuning sensitivity of the fill rate, one can deduce that the velocity of the LVIS beam was  $\sim 11$  m/s, which is consistent with the measurements of Wang and Buell [11] for our experimental parameters.

The number of molasses atoms measured as a function of load time is shown in Fig. 7. The fill curve was fit to  $N = a \cdot (1 - e^{-t/\tau})$ . The fit parameters were  $a = 1.1(1) \times 10^9$  atoms and  $\tau = 290(30)$  ms. The fill rate at short times gives the relevant fill rate of  $R_{t=0} = a/\tau = 3.8 \times 10^6$  atoms/ms. At this rate, it would require 24 ms to capture and launch  $10^7$  state-selected atoms. This loading rate is over two orders of magnitude larger than the loading rate for the optical molasses on our atomic fountain NIST-F1, which is loaded from a cesium oven. The total number of molasses atoms saturated at an intensity corresponding to  $5 \times I_{\text{sat}}$ . A higher intensity was required when the alignment of the molasses beams was not optimized. The fill rate at short times

implies that  $\sim 40\%$  of the LVIS atoms was being captured in the optical molasses.

The lifetime of the atoms in the molasses is 310(20) ms, which is about the same as the molasses fill rate. The decay time constant was measured by starting with a full molasses and then turning off the repump light to the MOT, which extinguishes the LVIS beam. The molasses was then held for some time before the number of remaining molasses atoms was measured. We attribute this decay mechanism to background collisions, since the diffusion time constant for an optical molasses is typically two orders of magnitude longer [12]. Background collisions reduce the apparent atom fill rate because some of the atoms that are captured in the molasses are lost through collisions before they are measured. Assuming that when a molasses atom collides with an atom from the background gas, it is scattered out of the molasses; if there were no background collisions, the fill rate would be two times higher than what we have observed, which would suggest that we capture 80% of the LVIS atoms instead of 40%. In any case, the level of agreement between the captured number and the LVIS flux is within the calibration uncertainties (50%) of the LVIS detection system. The observed lifetime is consistent with a background gas pressure of  $4 \times 10^{-8}$  mbar, which agrees with the pressure we find based on the current readings on the ion pump controllers (a few microamperes). This relatively high pressure for this system is understood and is the result of leaks caused by damage during transport of the apparatus. We are in the process of fixing this problem.

The optical molasses was not spherical, but was somewhat misshapen. We believe that the shape of the molasses was limited by the optics, and we cannot yet say how the asymmetric loading from the LVIS affects the molasses shape.

## V. DISCUSSION

A major challenge for NIST-F2 will be our goal for the reduction of the uncertainty in the spin exchange shift while achieving the stability level required to meet our goal of  $1 \times 10^{-16}$  for the combined total fractional uncertainty. We would like to operate the fountain most of the time with a stability of  $\sigma_y(\tau) = 1 \times 10^{-13}/\sqrt{\tau}$ . In our most recent NIST-F1 accuracy evaluation [2], while operating with a stability of  $\sigma_y(\tau) = 6 \times 10^{-13}/\sqrt{\tau}$ , we achieved an inaccuracy in the correction for the spin-exchange shift of  $1.5 \times 10^{-16}$ . The fountain stability is inversely proportional to  $\sqrt{N_d}$ , where  $N_d$  is the number of atoms detected at the end of a fountain cycle.

To meet our operational stability goal of  $\sigma_y(\tau) = 1 \times 10^{-13}/\sqrt{\tau}$  for NIST-F2, we need to increase  $N_d$  by almost a factor of 40 while we decrease the spin-exchange shift uncertainty by at least a factor of three. The huge atom load rates accessible with an LVIS will greatly expand the dynamic range of densities for atomic fountain operation, so achieving the factor of 40 increase in  $N_d$  should be possible. With the large load rates, we will be able to launch ten balls of atoms per cycle, so the atom number per ball will be increased from the typical number launched in NIST-F1 by a factor of four.

To control the size of the spin-exchange shift, for NIST-F2 we will increase the volume of the atom balls by about a factor of three over the ball volume currently used for NIST-F1. We

have experience with the advantages of launching larger balls in NIST-F1. Recently, we achieved a factor of three reduction of the spin-exchange uncertainty over previous evaluations mostly by increasing the horizontal molasses beam size such that the molasses volume was larger and the density was correspondingly lower for a given stability. In NIST-F1, the size of the up/down laser beams is restricted by the 1-cm aperture in the microwave cavities, so we could not increase the size of the two molasses beams that propagate along the flight tube. In NIST-F2, none of the molasses beams travel along the flight tube, and we expect to be able to increase the molasses volume by about an additional factor of two. We will also increase the aperture size in the microwave cavities from 10 mm to 12.5 mm so that fewer atoms are clipped in flight. The increase in total ball volume awarded with larger beams and cavity apertures means that the overall increase in the density required to meet our stability goal will be about 30%.

We will also be able to reduce the size of the relative error in the spin-exchange shift correction by a significant factor since we will be able to run at higher densities during the accuracy evaluation. For NIST-F1, the uncertainty of the spin-exchange shift is 28% of the total shift, and we are able to vary the density for the evaluation of the shift by a factor of five. With NIST-F2, we will have a better handle on the shift's density dependence since we will be able to evaluate the shift over a five times larger density range. With this longer baseline for extrapolating to zero density, we expect to reduce the uncertainty of the correction by a factor of five, which would put us below the  $3 \times 10^{-17}$  level for the spin-exchange uncertainty.

## ACKNOWLEDGMENT

The authors would like to thank E. Cornell, and C. Wieman for the use of the custom LVIS mirrors, G. Santarelli, T. Parker, and T. O'Brian for discussions, and N. Claussen, C. Langer, M. Lombardi, and D. Smith for valuable suggestions on this manuscript.

## REFERENCES

- [1] S. R. Jefferts, T. P. Heavner, E. A. Donley, J. H. Shirley, and T. E. Parker, "Second generation cesium fountain primary frequency standards at NIST," *Proc. IEEE IFCS*, pp. 1084–1088, May 2003.
- [2] T. P. Heavner, S. R. Jefferts, E. A. Donley, J. H. Shirley, and T. E. Parker, "Recent improvements in NIST-F1 and resulting accuracies of  $\delta f/f < 7 \times 10^{-16}$ ," in *Proc. IEEE CPEM Conf. Dig.*, 2004, pp. 498–499.
- [3] S. R. Jefferts, J. H. Shirley, T. E. Parker, T. P. Heavner, D. M. Meekhof, C. W. Nelson, F. Levi, G. Costanzo, A. DeMarchi, R. E. Drullinger, L. Hollberg, W. D. Lee, and F. L. Walls, "Accuracy evaluation of NIST-F1," *Metrologia*, vol. 39, pp. 321–336, 2002.
- [4] C. Fertig and K. Gibble, "Laser-cooled  $^{87}\text{Rb}$  Clock," *IEEE Trans. Instrum. Meas.*, vol. 48, no. 2, pp. 520–523, Apr. 1999.
- [5] G. Dudle, A. Joyet, P. Berthoud, G. Mileti, and P. Thomann, "First results with a cold cesium continuous fountain resonator," *IEEE Trans. Instrum. Meas.*, vol. 50, no. 2, pp. 510–514, Apr. 2001.
- [6] F. Levi, A. Godone, and L. Lorini, "Reduction of the cold collisions frequency shift in a multiple velocity fountain: A new proposal," *IEEE Trans. Ultrason., Ferroelectr., Freq. Contr.*, vol. 48, no. 3, pp. 847–850, May 2001.
- [7] F. Levi, A. Godone, L. Lorini, S. R. Jefferts, T. P. Heavner, and C. Calosso, "The multiple velocity fountain: A new scheme for the cold collision frequency shift reduction," in *Proc. Freq. Stand. Metrology Symp.*, 2001, pp. 466–468.

- [8] T. P. Heavner, L. Hollberg, S. R. Jefferts, J. Kitching, W. Kipstein, D. M. Meekhof, and H. G. Robinson, "Characterization of a cold cesium source for PARCS: Primary atomic reference clock in space," *IEEE Trans. Instrum. Meas.*, vol. 50, no. 2, pp. 500–502, Apr. 2001.
- [9] Z. T. Lu, K. L. Corwin, M. J. Renn, M. H. Anderson, E. A. Cornell, and C. E. Wieman, "Low-velocity intense source of atoms from a magneto-optical trap," *Phys. Rev. Lett.*, vol. 77, pp. 3331–3334, 1996.
- [10] C. Y. Park, M. S. Jun, and D. Cho, "Magneto-optical trap loaded from a low-velocity intense source," *J. Opt. Soc. Am. B.*, vol. 16, pp. 994–997, 1999.
- [11] H. Wang and W. F. Buell, "Velocity-tunable magneto-optical-trap-based cold Cs atomic beam," *J. Opt. Soc. Am. B.*, vol. 20, pp. 2025–2030, 2003.
- [12] H. J. Metcalf and P. van der Straten, *Laser Cooling and Trapping*. New York: Springer Verlag, 1999, pp. 87–97.
- [13] G. Santarelli, C. Audoin, A. Makdissi, P. Laurent, G. J. Dick, and A. Clairon, "Frequency stability degradation of an oscillator slaved to a periodically interrogated atomic resonator," *IEEE Trans. Ultrason., Ferroelectr., Freq. Contr.*, vol. 45, pp. 887–894, 1998.
- [14] H. R. Noh and W. Jhe, "Atom optics with hollow optical systems," *Phys. Rep.*, vol. 372, pp. 269–317, 2002.
- [15] K. Dieckmann, R. J. C. Spreeuw, M. Weidemüller, and J. T. M. Walraven, "Two-dimensional magneto-optical trap as a source of slow atoms," *Phys. Rev. A*, vol. 58, pp. 3891–3895, 1998.
- [16] A. Composteo, A. Piombini, F. Cervelli, F. Tantussi, F. Fusco, and E. Arimondo, "A cold cesium atomic beam produced out of a pyramidal funnel," *Opt. Commun.*, vol. 200, pp. 231–239, 2001.

**Elizabeth A. Donley** was born in Pueblo, CO, on April 5, 1970. She received the B.S. degree in physics from the University of Nevada, Las Vegas, in 1994 and the Ph.D. degree in natural sciences from the Swiss Federal Institute of Technology (ETH), Zürich, Switzerland, in 2000. Her Ph.D. work was in the field of single-molecule spectroscopy.

Upon receipt of the Ph.D. degree, she became a Postdoctoral Fellow at the University of Colorado/JILA, Boulder, in Bose–Einstein condensation. She has been a Permanent Staff Physicist at the National Institute of Standards and Technology (NIST), Boulder, since 2002, where she is a member of the Atomic Standards Group.

**Thomas P. Heavner** was born in Alexandria, VA, on October 28, 1966. He received the B.S. degree in physics from the University of Virginia, Charlottesville, in 1989 and the Ph.D. degree from the University of Colorado/JILA, Boulder, in 1998. His Ph.D. work involved precision mass measurements of single Li ions using a Penning Trap apparatus.

Upon receipt of the Ph.D. degree, he became an NRC Postdoctoral Fellow in the Time and Frequency Division of the National Institute of Standards and Technology (NIST), Boulder. In 2001, he became a Permanent Staff Member at NIST in the Atomic Standards Group.

**Steven R. Jefferts** (M'01) received the B.S. degree in physics from the University of Washington, Seattle, in 1984 and the Ph.D. degree in atomic physics/precision metrology from the University of Colorado, Boulder, in 1992.

He then went to the National Institute of Standards and Technology (NIST), Boulder, as an NRC Postdoctoral Fellow, where he worked on trapped laser-cooled ions. He joined NIST as a Permanent Staff Member in 1994, and presently works on primary frequency standards.

Dr. Jefferts was the 2004 Distinguished Lecturer of the IEEE Ultrasonics, Ferroelectrics, and Frequency Control Society.